Subthalamic and Pallidal Stimulations in Patients with Parkinson's Disease: Common and Dissociable Connections

Chencheng Zhang, MD, PhD ,[1,2,3,4†] Yijie Lai, MD ,[1,2†] Jun Li, PhD ,[1,2,5†]
Naying He, MD, PhD,[6] Yu Liu, MD,[6] Yan Li, MS,[6] Hongyang Li, MD,[1,2]
Hongjiang Wei, PhD,[7,8] Fuhua Yan, MD, PhD,[6] Andreas Horn, MD, PhD ,[9]
Dianyou Li, MD, PhD,[1,2] and Bomin Sun, MD, PhD[1,2]

Objective: The subthalamic nucleus (STN) and internal globus pallidus (GPi) are the most effective targets in deep brain stimulation (DBS) for Parkinson's disease (PD). However, the common and specific effects on brain connectivity of stimulating the 2 nuclei remain unclear.

Methods: Patients with PD receiving STN-DBS (n = 27, 6 women, mean age 64.8 years) or GPi-DBS (n = 28, 13 women, mean age 64.6 years) were recruited for resting-state functional magnetic resonance imaging to assess the effects of STN-DBS and GPi-DBS on brain functional dynamics.

Results: The functional connectivity both between the somatosensory-motor cortices and thalamus, and between the somatosensory-motor cortices and cerebellum decreased in the DBS-on state compared with the off state ($p < 0.05$). The changes in thalamocortical connectivity correlated with DBS-induced motor improvement ($p < 0.05$) and were negatively correlated with the normalized intersection volume of tissues activated at both DBS targets ($p < 0.05$). STN-DBS modulated functional connectivity among a wider range of brain areas than GPi-DBS ($p = 0.009$). Notably, only STN-DBS affected connectivity between the postcentral gyrus and cerebellar vermis ($p < 0.001$) and between the somatomotor and visual networks ($p < 0.001$).

Interpretation: Our findings highlight common alterations in the motor pathway and its relationship with the motor improvement induced by both STN- and GPi-DBS. The effects on cortico-cerebellar and somatomotor-visual functional connectivity differed between groups, suggesting differentiated neural modulation of the 2 target sites. Our results provide mechanistic insight and yield the potential to refine target selection strategies for focal brain stimulation in PD.

ANN NEUROL 2021;90:670–682

Parkinson's disease (PD) is a neurodegenerative disorder primarily resulting from the death of dopaminergic neurons in the substantia nigra and characterized by widespread progressive brain pathology; however, knowledge

regarding dysfunction at the neural circuit level remains uncertain. The traditional model[1] of the motor circuit and its alteration in PD conceptualized in the late 1980s highlighted modulation of the disrupted balance of the basal ganglia as the primary therapeutic means for PD.

Deep brain stimulation (DBS) targeting either the subthalamic nucleus (STN) or internal globus pallidus (GPi) stimulation can improve both motor symptoms and quality of life.[2] Although stimulating either target similarly impacts many primary motor outcomes, STN-DBS appears to facilitate a larger reduction in dopaminergic medication, which has been associated with a potential risk of cognitive and mood decline. In contrast, GPi-DBS shows better antidyskinetic effects and fewer adverse effects related to speech, swallowing, and gait difficulties than STN-DBS.[2,3] Therefore, DBS targeting STN and GPi may have a common, but partly specific, effect on brain network activities.

DBS has also expanded our understanding of brain circuitry. Several functional magnetic resonance imaging (fMRI) studies have investigated the dynamic brain changes induced by STN-DBS. STN-DBS leads to altered activity in motor-related areas, including the motor cortices, basal ganglia, thalamus, and cerebellum.[4–8] Subthalamic stimulation elevates the degree of centrality in the bilateral motor cortices and affects the connectivity of these motor hubs with the thalamus and cerebellum.[9–13] STN-DBS also shifts the global brain dynamics of patients with PD toward those of healthy controls.[14,15] However, the common and specific effects of subthalamic and pallidal stimulations on the brain network remain unclear. Animal studies have suggested a difference in the DBS effects targeting the 2 nuclei, with 1 animal study suggesting STN-DBS would impact a wider range of brain areas than GPi-DBS,[16] and another suggesting GPi-DBS would have a different effect on the contralateral hemisphere.[17]

Based on studies on monkeys, the therapeutic effects of STN-DBS or GPi-DBS are proposed to be mediated by modulation of neural activity in the motor thalamus and cortex.[18] The motor thalamus mainly consists of the ventrolateral nucleus and the ventroanterior nucleus, whose neurons are primarily glutamatergic and predominantly project onto pyramidal neurons in the cerebral cortex,[19] receive inputs from the basal ganglia and cerebellum, and then reciprocally transfer the signal to the cortex.[20] Other explanatory concepts have been proposed to this end, and the effects of DBS are applied to either target propagate via distributed brain networks.[14,16]

In the present study, we primarily examined changes in functional connectivity in patients with PD to explore the neurotherapeutic mechanisms underlying subthalamic and pallidal stimulations. Furthermore, we examined the common and specific effects of DBS at these 2 target sites on the functional connectivity between motor-related regions of interest, as well as nonmotor networks, to strengthen our understanding of the neural mechanisms underlying the common but differentiated clinical observations.

Materials and Methods

Recruitment and Criteria

Patients with PD who had previously undergone STN- or GPi-DBS at Ruijin Hospital were recruited by telephone by neurosurgeons from September 2019 to December 2020. Right-handed patients aged 45 to 75 years with idiopathic PD who received 2 quadripolar DBS electrodes (Medtronic 3387, Medtronic, USA; or SceneRay 1210, SceneRay, China) were included. We excluded patients with an excessive tremor in DBS-off and medication-off states, other serious psychiatric disorders (eg, schizophrenia and bipolar disorder) meeting DSM-5 criteria, other major neurological illnesses, unstable vital signs, or any postoperative complications detected using postoperative MRI. The ethics committee of Ruijin Hospital approved all procedures (Approval Number: 2018017) in the present study. All patients provided written informed consent according to the Declaration of Helsinki. More than 20 participants for STN-DBS and GPi-DBS, respectively, were recruited because a sample size ≥20 is recommended for sufficient reliability in functional neuroimaging studies.[21]

Clinical Evaluation

The study protocol is illustrated in Figure 1. Experienced neurologists performed primary clinical assessments via telephone a few days before scanning. On the day of scanning, motor function in the DBS-on state was first evaluated by a movement disorder specialist using the Movement Disorder Society's Unified Parkinson's Disease Rating Scale-III (MDS UPDRS-III)[22] after overnight medication withdrawal. After DBS-on scanning, the DBS was switched off, and the participants waited for an hour or until the motor symptoms re-appeared. Then, motor function was evaluated for the second time, immediately after which DBS-off scanning was performed.

MRI Data Acquisition

Postoperative T1 images and resting-state functional images were acquired using a 1.5-T MRI machine (Aero, Siemens, Germany). The postoperative T1 MP-RAGE images were acquired with the following parameters: repetition time $=$ 3400 ms, echo time $=$ 3 ms, inversion time $=$ 900 ms, flip angle $=$ 8°, voxel size $=$ $1.0 \times 1.0 \times 1.0$ mm^3, matrix $=$ 224 × 216, and number of slices $=$ 192. The resting-state functional MR EPI images were acquired with the following parameters: 210 volumes, repetition time $=$ 2100 ms, echo time $=$ 40 ms, flip angle $=$ 90°, voxel size $=$ $3.0 \times 3.0 \times 3.0$ mm^3, gap $=$ 0.9 mm, matrix $=$ 66 × 66, and number of slices $=$ 37. T1 MP-RAGE images acquired before DBS implantation were downloaded
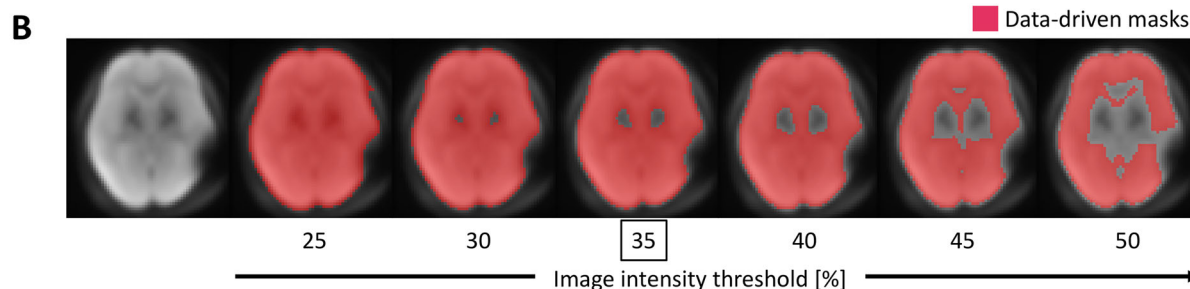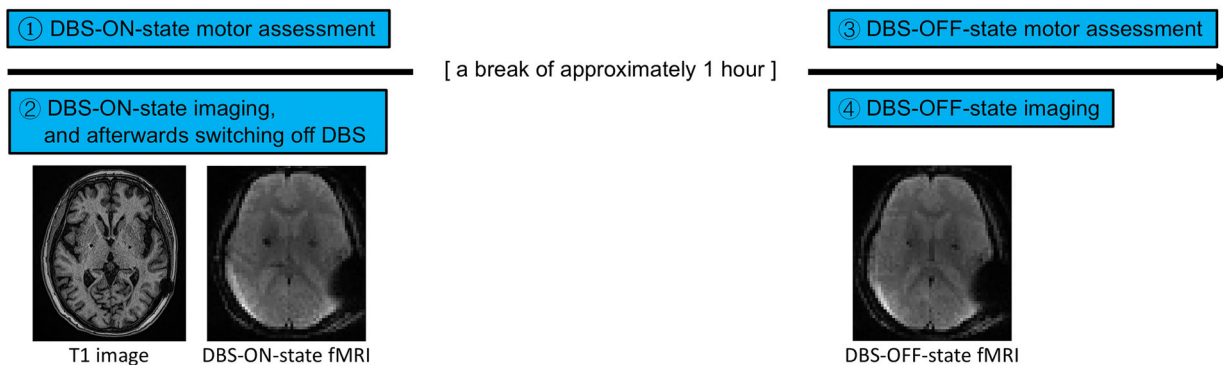
A [overnight withdrawal of medication the day before]

① DBS-ON-state motor assessment   ③ DBS-OFF-state motor assessment

[a break of approximately 1 hour]

② DBS-ON-state imaging,
and afterwards switching off DBS   ④ DBS-OFF-state imaging

T1 image   DBS-ON-state fMRI   DBS-OFF-state fMRI

B   Data-driven masks

25   30   35   40   45   50

Image intensity threshold [%]

FIGURE 1: Study procedure and data-driven masking procedure. (A) Study procedure. (B) Data-driven masking procedure based on image intensity to account for magnetic susceptibility artifacts caused by the metallic DBS electrodes and the pulse generator. Various image intensity thresholds ranging from 25% to 50% with a step size of 5% were used for qualitative assessment of the artifacts and formation of the mask for subsequent calculations. The masks were overlaid on an average normalized post-surgery fMRI scan. After visual inspection, a moderate threshold of 35% was chosen as the mask. DBS = deep brain stimulation; fMRI = functional magnetic resonance imaging. [Color figure can be viewed at www.annalsofneurology.org]

from the medical database of the hospital. The preoperative T1 images were acquired on a 3.0-T MRI machine (HXDt; General Electric, Boston, MA) with the following parameters: repetition time = 6.48 ms, echo time = 2 ms, inversion time = 450 ms, flip angle = 15°, voxel size = $0.47 \times 0.47 \times 1.0$ mm^3, matrix = 512×512, and number of slices = 144.

DBS Position Reconstruction and Volumes of Tissue Activated Calculation

DBS placement was reconstructed using the Lead-DBS toolbox[23] (version 2.3.2; www.lead-dbs.org) implemented in MATLAB (version 2017a; The MathWorks, Natick, MA). First, the post-operative T1 image was coregistered to the pre-operative T1 image using SPM (https://www.fil.ion.ucl.ac.uk/spm/software/spm12/).[24] Brain shift correction was performed with a coarse-plus-fine mask to further refine the subcortical target regions of interest on the post- and preoperative T1 images,[25] thus minimizing the nonlinear bias introduced during skull opening while in surgery. Then, the images were normalized into the ICBM 2009b Nonlinear Asymmetric[26] Montreal Neurological Institute (MNI) space with the symmetric diffeomorphic registration algorithm implemented in Advanced Normalization Tools[27] (http://stnava.github.io/ANTs/) using the "effective (low variance)" preset with subcortical refinement as implemented in Lead-DBS.[23] Thereafter, electrodes were automatically pre-localized and manually adjusted using Lead-DBS. The volumes of tissue activated

(VTAs) were further modeled using a finite element approach[23,28] implemented in Lead-DBS using default parameters. Finally, VTA and atlas-defined masks of interest (STN or GPi)[29] intersections were generated.

Functional Imaging Data Preprocessing

Resting-state fMRI data were processed using the Data Processing and Analysis of Brain Imaging (DPABI) toolbox (version 4.1; http://rfmri.org/dpabi).[30] The first 10 volumes of functional images were excluded to eliminate unstable data. After slice timing correction, the images were realigned to correct for head movement. The functional images were normalized to the MNI space using the method of Diffeomorphic Anatomical Registration Through Exponentiated Lie Algebra.[31] Spatial smoothing was performed with a gaussian kernel of $6 \times 6 \times 6$ mm^3 full-width at half maximum. White matter and cerebrospinal fluid signals and Friston 24 head motion parameters[32] were regressed out as nuisance covariates. A bandpass filter was used to extract signals between 0.009 and 0.08 Hz.

Voxel-Wise Degree Centrality

The common mask was created by an intensity cutoff-threshold of 35% (see Fig 1) to exclude fMRI voxels exhibiting severe magnetic susceptibility artifacts caused by the DBS apparatus.[11] The value of degree centrality was calculated using DPABI. The blood-oxygen-level-dependent (BOLD) time course of each voxel

TABLE. Demographics, Clinical Characteristics, and Stimulation Parameters

	Patients with STN-DBS	Patients with GPi-DBS	Between-group comparison
n	27	28	
Age (yr)	64.8 (7.6)	64.6 (9.0)	$t = 0.089$, $p = 0.929$
Sex ratio (male/female)	21/6	15/13	$X^2 = 3.562$, $p = 0.059$
Disease duration (yr)	11.7 (4.2)	11.1 (4.0)	$t = 0.542$, $p = 0.590$
Levodopa response before DBS surgery (%)	41.8 (12.6)	39.2 (20.0)	$t = 0.500$, $p = 0.621$
Period after DBS implantation surgery (mo)	10.0 (4.6)	21.3 (8.9)	$t = 5.945$, $p < 0.001$
Dosage of levodopa equivalent (mg/day)	821.8 (571.4)	834.1 (388.5)	$t = 0.093$, $p = 0.926$
DBS voltage – left electrode (volts)	2.7 (0.5)	3.3 (0.5)	$t = 4.449$, $p < 0.001$
DBS frequency – left electrode (Hz)	120.0 (26.8)	145.7 (15.4)	$t = 4.340$, $p < 0.001$
DBS pulse width – left electrode (μs)	67.0 (11.7)	70.0 (11.2)	$t = 0.971$, $p = 0.336$
DBS voltage – right electrode (volts)	2.6 (0.5)	3.2 (0.4)	$t = 4.903$, $p < 0.001$
DBS frequency – right electrode (Hz)	119.3 (27.1)	145.9 (15.2)	$t = 4.467$, $p < 0.001$
DBS pulse width – right electrode (μs)	64.1 (8.4)	66.1 (9.6)	$t = 0.823$, $p = 0.414$
DBS-off state MDS UPDRS-III (medication-off state)	54.3 (16.2)	53.3 (12.7)	$t = 0.254$, $p = 0.800$
DBS-on state MDS UPDRS-III (medication-off state)	32.9 (10.9)	40.6 (14.3)	$t = 2.251$, $p = 0.029$

Note: Values are reported as mean (standard deviation). The average levodopa response (levodopa challenge test) before surgery was calculated from the records of 26 patients with STN-DBS and 19 patients with GPi-DBS.

Abbreviations: DBS = deep brain stimulation; GPi = internal globus pallidus; MDS UPDRS = Movement Disorders Society Unified Parkinson's Disease Rating Scale; STN = subthalamic nucleus.
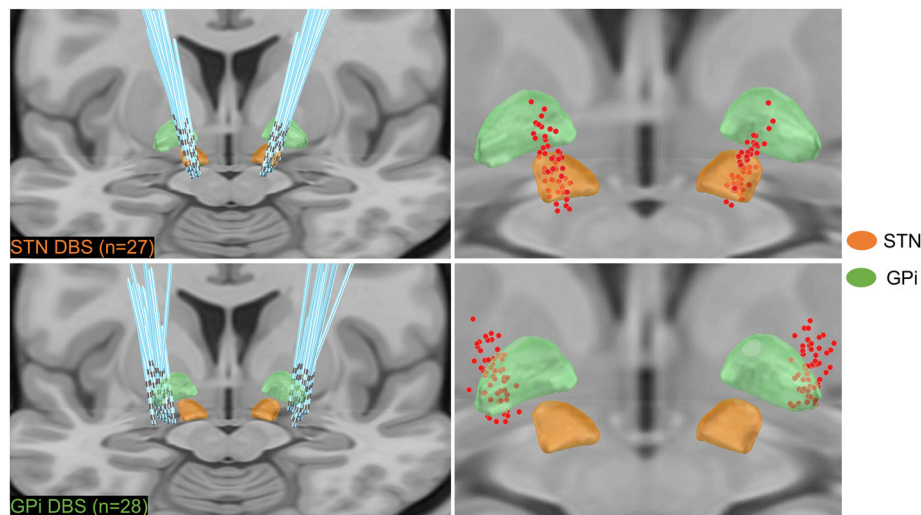

FIGURE 2: Position of electrodes reconstructed using Lead-DBS with STN and GPi as DBS target sites. Upper panel: STN-DBS electrode position (n = 27); lower panel: GPi-DBS electrode position (n = 28). Red dots indicate the position of the active contacts. STN in orange; GPi in green. DBS = deep brain stimulation; GPi = internal globus pallidus; STN = subthalamic nucleus.
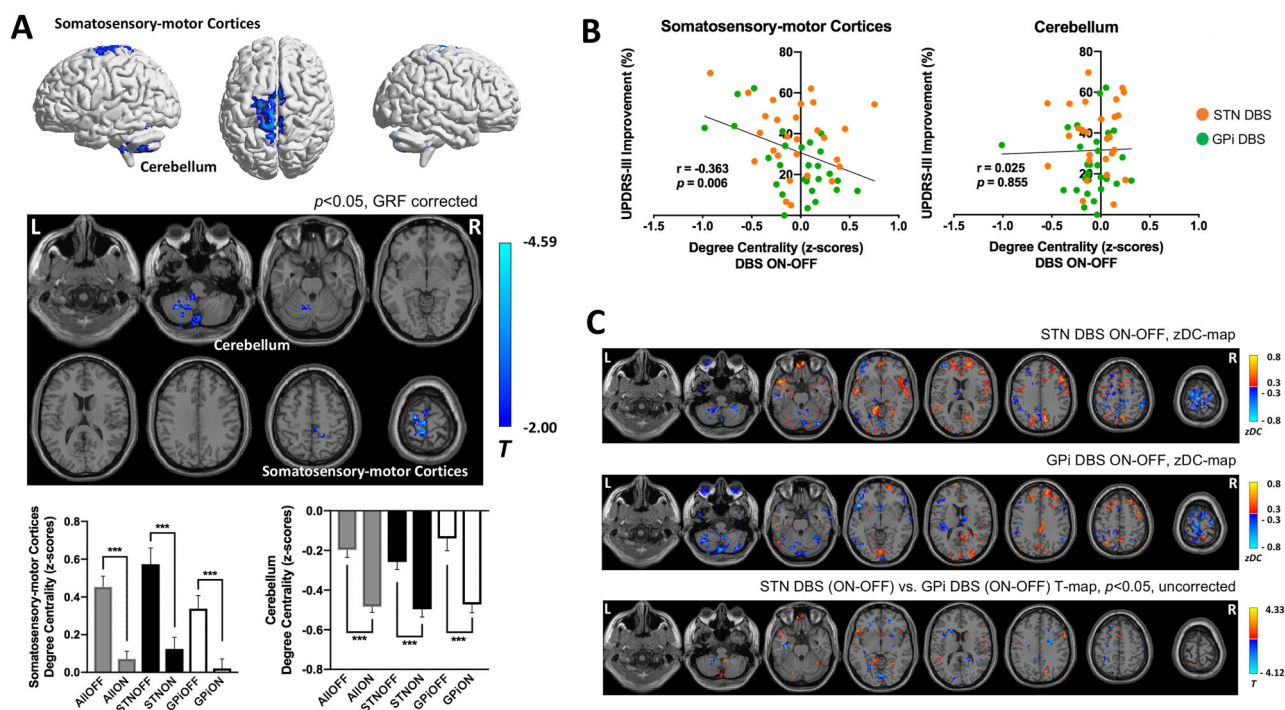
FIGURE 3: Alterations in degree centrality induced by DBS. (A) Brain areas showing significant decreases of degree centrality (blue color) in a voxel-wise analysis, regardless of target (STN and GPi combined; analysis corrected for target group). There were no significant increases of degree centrality induced by DBS. (B) Alterations of degree centrality were correlated with motor improvement by DBS in the somatosensory-motor cortices, but not in the cerebellum. (C) A comparison of DBS-induced alterations in degree centrality between the targets. There were no significant differences of alterations in degree centrality between the targets after correction for multiple comparisons. UPDRS = Unified Parkinson's Disease Rating Scale; DBS = deep brain stimulation; STN = subthalamic nucleus; GPi = internal globus pallidus; GRF = Gaussian random field; DC = degree centrality.

was extracted, and its Pearson correlation coefficients with every other voxel in the common mask calculated. Based on these, average connectivity between each voxel and all other voxels was calculated as the weighted version of degree centrality (strength centrality),[33] used as an index to measure the changes in the voxel-wise functional connectivity induced by STN-DBS.[14]

Seed-Based Functional Connectivity

The brain area whose degree centrality alters and shows correlation with motor improvement by DBS (ie, somatosensory-motor cortices; see the Results section) was chosen as the seed region. Seed-based functional connectivity was calculated between the averaged time course of all voxels within the seed and each of the voxels within the common mask using DPABI, and Fisher's r-to-z transformation was used to improve the normality of the connectivity values. Besides the voxel-wise analysis, regions-of-interest (ROI) analyses were also performed. The first ROI analysis included 9 motor-related regions within the cortico-basal ganglia-thalamocortical circuit and the cerebellum chosen from Anatomical Automatic Labeling Atlas 3,[34] and functional connectivity between each pair of regions was calculated for both DBS-on and DBS-off states. The motor-related ROIs included the supplementary motor area, precentral gyrus, postcentral gyrus, paracentral lobule, caudate, putamen, motor thalamus, cerebellum hemispheres, and vermis (Supplementary Table S1). The second ROI analysis included 7 cortical functional network parcellations based on intrinsic functional connectivity created by Yeo and

colleagues, together with the subcortical structures of basal ganglia, thalamus and cerebellum (Supplementary Table S2). The brain parcellation ROIs consisted of the default-mode network, somatomotor network, dorsal-attention network, ventral-attention network, limbic network, frontoparietal network, and visual network. The analysis with inclusion of the brain parcellation ROIs outside the motor-related regions examined whether a difference in functional connectivity among nonmotor regions exists between STN- and GPi-DBS.

Outcomes

Alterations in functional connectivity (both degree centrality and seed-based functional connectivity) induced by DBS, and the relationship between motor function improvement induced by DBS and the alterations in functional connectivity were examined. Additionally, the common and specific changes in functional connectivity between each pair of regions of interest induced by the 2 types of DBS were examined.

Statistical Analysis

Continuous variables are presented as mean (standard deviation) values. Statistical analysis was performed with SPSS (version 25; IBM Corp., Armonk, NY) and result graphs presented using GraphPad Prism (version 8.0; GraphPad Software, San Diego, CA). Differences between STN-DBS and GPi-DBS groups were examined using independent-samples t test or the Chi-squared test. The alteration between the DBS-on state and -off state was
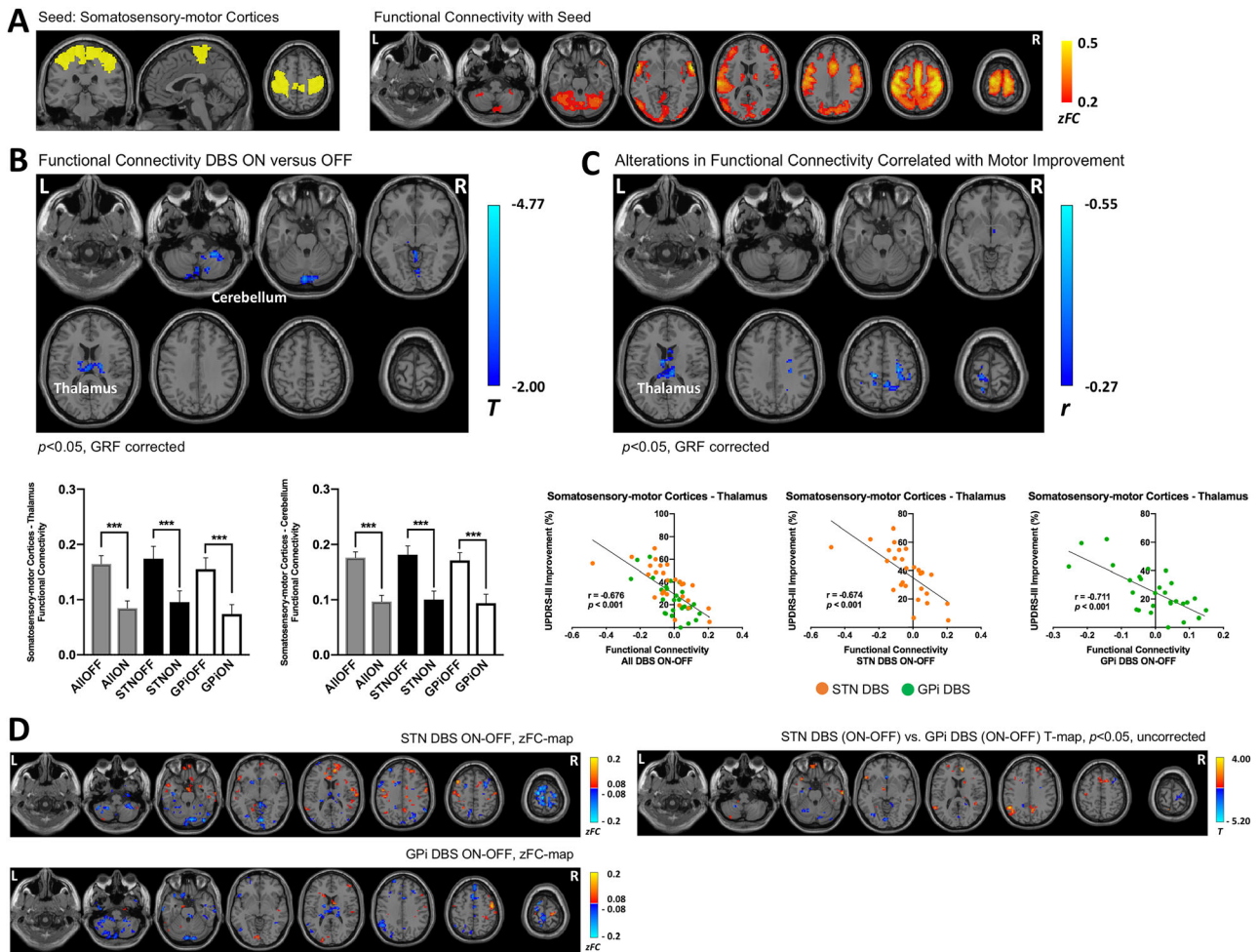
FIGURE 4: Somatosensory-motor cortex-seeded functional connectivity altered by DBS. (A) Brain areas showing functional connectivity to the somatosensory-motor cortices (yellow region). (B) Brain areas showing significant decrease of functional connectivity (blue color) in a voxel-wise analysis, regardless of target (STN and GPi combined; analysis corrected for target group). There were no significant increases of functional connectivity induced by DBS. (C) Brain areas in which the functional connectivity significantly correlated with changes in UPDRS-III scores under DBS (blue color indicates negative correlation); significant positive changes not observed. (D) A comparison of DBS-induced alterations in functional connectivity between the targets. There were no significant differences of alterations in functional connectivity between the targets after correction for multiple comparisons. DBS = deep brain stimulation; FC = functional connectivity; GPi = internal globus pallidus; GRF = Gaussian random field; STN = subthalamic nucleus; UPDRS = Unified Parkinson's Disease Rating Scale.

examined using paired-samples t test. Pearson's correlation analysis was used to reveal the voxels where functional connectivity alterations (DBS-on state vs -off state) significantly correlated with clinical changes on the motor part of the UPDRS-III. Imaging results were considered significant at an alpha level of $p < 0.05$ (2-tailed) after correction for multiple comparisons using the gaussian random field (GRF) method embedded in the Viewer module of DPABI.[30] The resulting voxel-wise maps were overlaid on rendering views with BrainNet Viewer (version 1.7; https://www.nitrc.org/projects/bnv/) or on axial slice views with the Viewer module of DPABI.

Data Availability
The DBS MRI datasets generated and analyzed during the current study are not publicly available because of data privacy regulations of patient data but are available from the corresponding authors upon reasonable request.

Results

Demographics and Clinical Measurements
Twenty-seven patients with PD who underwent STN-DBS and 28 patients who underwent GPi-DBS were included. The age, sex, means of disease duration, the period after DBS implantation surgery, the daily dosage of levodopa equivalent, DBS parameters, and MDS-UPDRS-III scores with DBS on and DBS off in the medication-off state are presented in the Table. The individual stimulation parameters presented in Supplementary Table S3. The total scores on UPDRS-III and the scores on 4 major
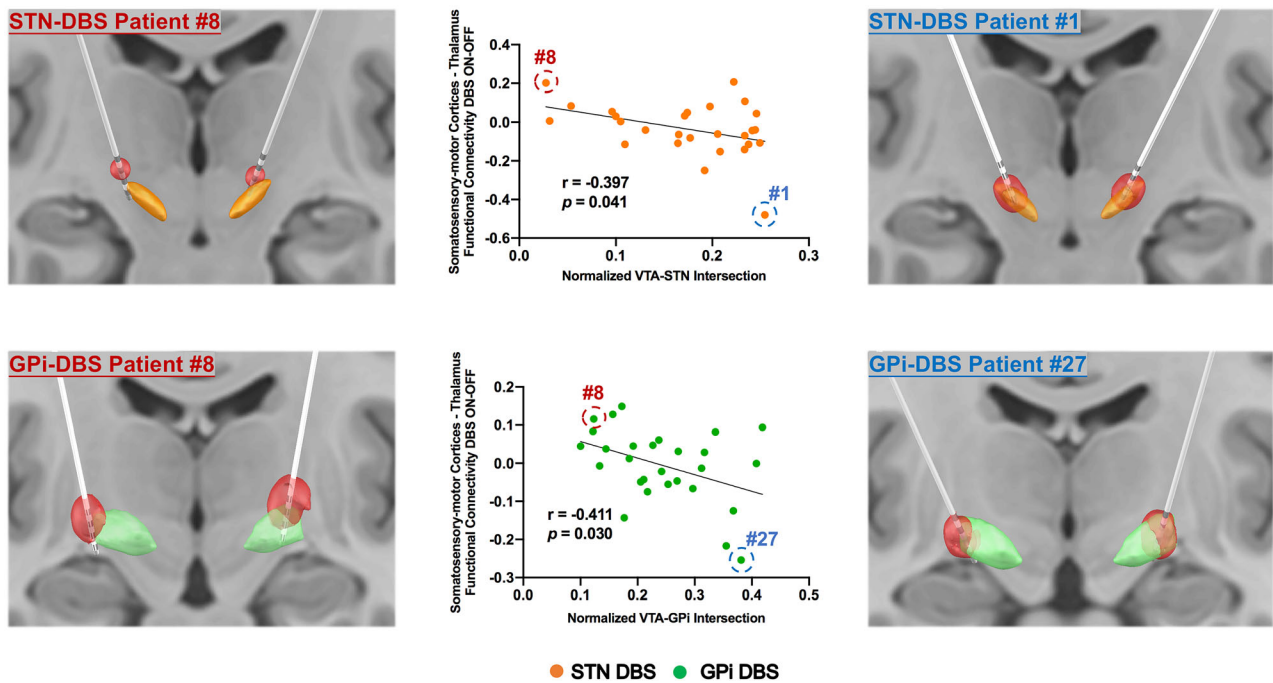
FIGURE 5: Modulation of somatosensory-motor cortex-thalamus connectivity using VTA-nucleus intersection. Changes in functional connectivity between the somatosensory-motor cortices and thalamus of the DBS-on versus -off state significantly correlated with normalized intersection volumes between estimated VTAs and the anatomic extent of the nucleus in both STN-DBS and GPi-DBS. DBS = deep brain stimulation; GPi = internal globus pallidus; UPDRS = Unified Parkinson's Disease Rating Scale; VTA = volumes of tissue activated. [Color figure can be viewed at www.annalsofneurology.org]

symptoms (rigidity, tremor, bradykinesia, and axial)[35] were not significantly different between the STN-DBS group and the GPi-DBS group in the DBS-off state (Supplementary Table S4).

Alterations in Degree Centrality Induced by DBS

The electrode position reconstructed using Lead-DBS is shown in Figure 2. The voxel-wise analysis indicated that the degree centrality decreased in the somatosensory-motor cortices and cerebellum ($p < 0.05$, GRF corrected, Fig 3A; Supplementary Table S5). Changes in degree centrality of the somatosensory-motor cortices between DBS-on versus DBS-off states negatively correlated with the improvement in MDS-UPDRS-III scores of the DBS-on state versus DBS-off state (Fig 3B). Such a correlational relationship was not observed in the cerebellum (see Fig 3B). A comparison of DBS-induced alterations in degree centrality between the targets was made (Fig 3C). No brain areas showed interaction in degree centrality between the STN-DBS group and the GPi-DBS group after GRF correction. The mean of framewise displacement of the STN-DBS group (DBS on = 0.14 ± 0.11 mm; DBS off = 0.09 ± 0.08 mm) was not statistically different from that of the GPi-DBS group (DBS on = 0.09 ± 0.07 mm; DBS off = 0.09 ± 0.06 mm).

Thalamocortical Functional Connectivity Associated with Motor Improvement

The voxel-wise functional connectivity indicated that the somatosensory-motor cortices were functionally connected to a wide range of cortical and subcortical areas (Fig 4A), including the motor-related cortices, thalamus, and cerebellum. The thalamus and cerebellum showed decreased functional connectivity with somatosensory-motor cortices between DBS-on versus DBS-off states (Fig 4B; Supplementary Table S6). Changes in functional connectivity between the thalamus and somatosensory-motor cortices induced by DBS negatively correlated with the improvement in MDS-UPDRS-III scores of the DBS-on state versus DBS-off state in both patients with STN-DBS and those with GPi-DBS ($p < 0.05$, GRF corrected, Fig 4C; Supplementary Table S7). A comparison of DBS-induced alterations in functional connectivity between the targets was made (Fig 4D). No difference in DBS-induced changes in functional connectivity seeding from the somatosensory-motor cortices was observed between the 2 groups after correction for multiple comparisons.

Thalamocortical Functional Connectivity Modulated with VTA-Nucleus Intersection

In the next step, we measured whether the amount of overlap between stimulation volumes (as estimated with VTA) and the target structure could explain changes in
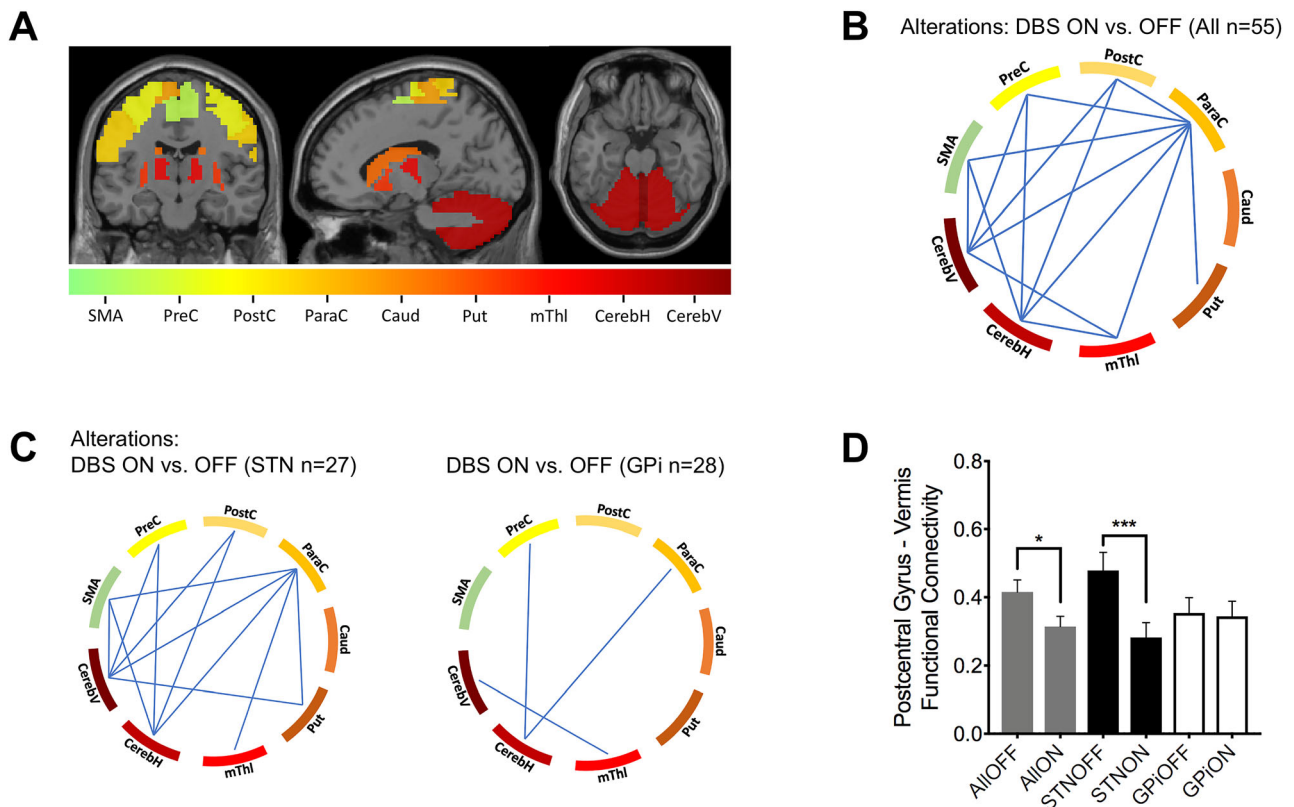
FIGURE 6: Common and differentiated changes in functional connectivity among the motor-related regions following STN- and GPi-DBS. (A) Motor-related regions of interest. (B) The difference in functional connectivity between the DBS-on state and -off state for the pairs of regions of interest. Blue lines indicate a statistically significant decrease in value (p < 0.05). (C) The difference in functional connectivity between the DBS-on state and -off state for the pairs of regions of interest under STN-DBS and GPi-DBS. (D) The significant interactions between the alterations induced by STN-DBS and GPi-DBS. While STN-DBS significantly decreased the functional connectivity between the postcentral gyrus and the vermis, the GPi-DBS effect did not alter this connectivity. Error bars indicate standard error of the mean. *p < 0.05; ***p < 0.001. Caud = caudate; CerebH = cerebellum hemisphere; CerebV = cerebellum vermis; DBS = deep brain stimulation; GPi = internal globus pallidus; mThl = motor thalamus; ParaC = paracentral lobule; PostC = postcentral gyrus; PreC = precentral gyrus; Put = putamen; SMA = supplementary motor area; STN = subthalamic nucleus.

thalamocortical connectivity. The changes in thalamocortical connectivity significantly correlated with the normalized intersection volume of VTA and targeted nucleus in both patients with STN- and GPi-DBS (STN-DBS group: $r = -0.379$, $p = 0.041$; GPi-DBS group: $r = -0.411$, $p = 0.030$; Fig 5). Such correlations were not significant after regressing out the covariate effect of motor improvement induced by DBS (STN-DBS group with UPDRS-III total scores as the covariate: $r = -0.217$ and $p = 0.287$; GPi-DBS group with UPDRS-III total scores as the covariate: $r = -0.233$ and $p = 0.241$).

Further DBS-Induced Connectivity Changes under STN- and GPi-DBS

Besides the voxel-wise analysis, we performed ROI analysis to reveal the DBS-induced connectivity changes and the interaction of connectivity modulated by STN-DBS versus GPi-DBS. As mentioned in the Methods section, 2 ROI analyses were performed, one with the motor-related ROIs,

and the other with the functional network parcellations (including the nonmotor regions) and subcortical structures. Functional connectivity between pairs of motor-related ROIs (Fig 6A) revealed that DBS at the STN or GPi significantly reduced functional connectivity among motor-related cortical and subcortical regions ($p < 0.05$; Fig 6B, Supplementary Table S8). The DBS-induced decrease in connectivity was observed in more extensive regions in patients with STN-DBS (12 pairs of regions in patients with STN-DBS vs. 3 pairs of regions in patients with GPi-DBS, X^2 (1) = 6.821, $p = 0.009$; Fig 6C, Supplementary Table S8), and a significant interaction was observed between the DBS effect and functional connectivity between the postcentral gyrus and the cerebellar vermis ($t(53) = 2.486$, $p = 0.016$). Although STN-DBS significantly weakened the functional connectivity between the postcentral gyrus and vermis ($p < 0.001$), the GPi-DBS did not alter this connectivity ($p = 0.860$) (Fig 6D). The functional connectivity between the postcentral gyrus and the
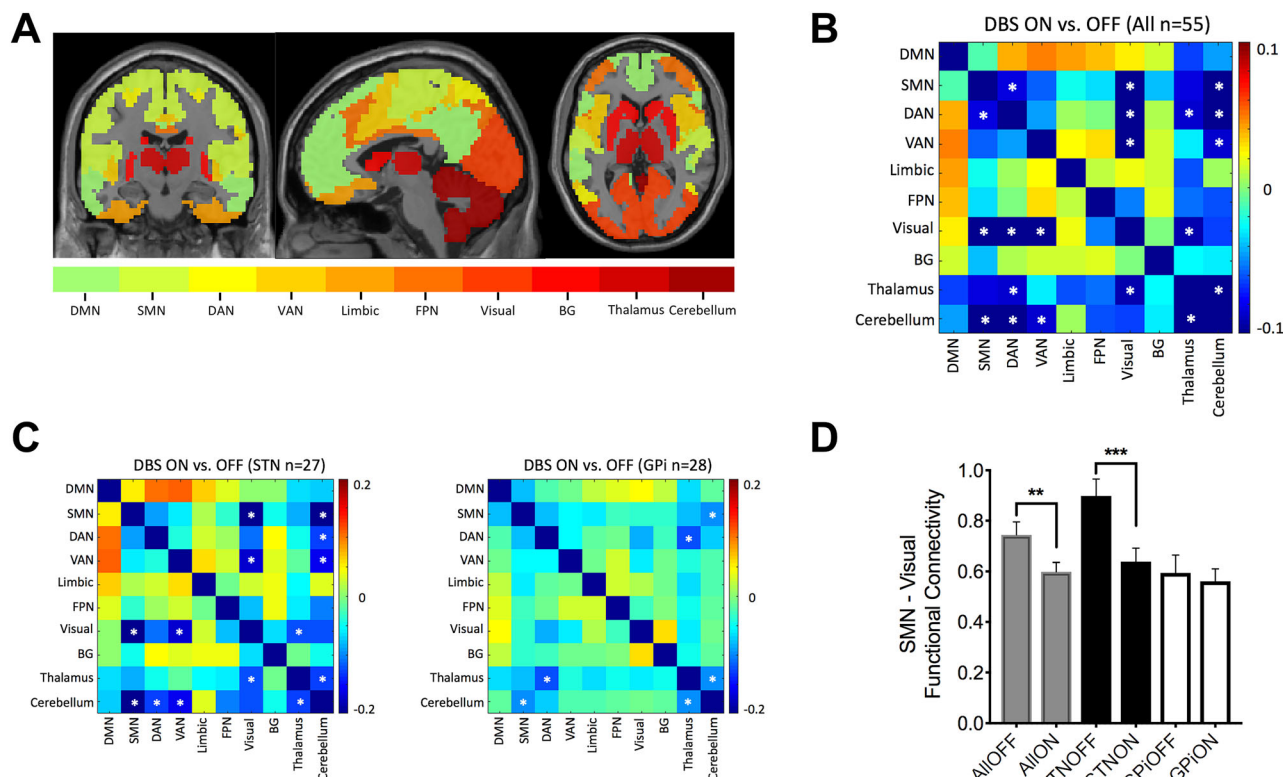
FIGURE 7: Common and differentiated changes in functional connectivity among the brain networks and subcortical regions following STN- and GPi-DBS. (A) Brain networks and subcortical regions of interest. (B) The difference in functional connectivity between the DBS-on state and -off state for the pairs of regions of interest. White stars indicate a statistically significant decrease in value (*p* < 0.05). (C) The difference in functional connectivity between the DBS-on state and -off state for the pairs of regions of interest under STN-DBS and GPi-DBS. (D) The significant interactions between the alterations induced by STN-DBS and GPi-DBS. While STN-DBS significantly decreased the functional connectivity between the postcentral gyrus and the vermis, the GPi-DBS effect did not alter this connectivity. Error bars indicate standard error of the mean. ****p* < 0.01; ***p* < 0.001.* BG = basal ganglia; DBS = deep brain stimulation; DAN = dorsal attention network; DMN = default-mode network; FPN = frontoparietal network; GPi = internal globus pallidus; SMN = somatomotor network; STN = subthalamic nucleus; VAN = ventral attention network.

cerebellar vermis significantly correlated with the UPDRS-III total score ($r = -0.315$ and $p = 0.019$), but not with the rigidity score ($r = -0.139$ and $p = 0.310$). The inclusion of motor improvement as an covariate slightly influenced the significance level of the interaction between stimulation targets (UPDRS-III total score included as the covariate: $F(1, 54) = 2.971$ and $p = 0.091$; rigidity score included as the covariate: $F(1, 54) = 4.926$ and $p = 0.031$). Similarly, functional connectivity between multiple pairs of cortical and subcortical parcellations, including nonmotor areas (Fig 7A), decreased with DBS (Fig 7B). The DBS-induced decrease in connectivity was observed in more extensive regions in patients with STN-DBS (Fig 7C; Supplementary Table S9). Significant interactions between the 2 therapies were found in the connectivity between the somatomotor network and visual network ($t(53) = 2.448$ and $p = 0.018$). Whereas STN-DBS significantly weakened the functional connectivity between the somatomotor network and visual network ($p < 0.001$), the GPi-DBS effect did not alter this

connectivity ($p = 0.545$; Fig 7D). The functional connectivity between the somatomotor network and the visual network significantly correlated with the UPDRS-III total score ($r = -0.304$ and $p = 0.024$), but not with the rigidity score ($r = -0.217$ and $p = 0.111$). The inclusion of motor improvement as a covariate slightly influenced the significance level of this interaction between the stimulation targets (UPDRS-III total score included as the covariate: $F(1, 54) = 2.964$ and $p = 0.091$; rigidity score included as the covariate: $F(1, 54) = 3.487$ and $p = 0.068$).

Discussion

Multiple recent studies have investigated the changes in fMRI data under DBS targeting the STN in patients with PD. However, the changes in functional connectivity under GPi-DBS, particularly the common and dissociable effects induced by DBS at the 2 nuclei on brain connectivity, remain unclear. Here, we investigated the impact

on functional connectivity by both STN-DBS and GPi-DBS to strengthen the understanding of the neural mechanisms underlying the common but differentiated clinical observations.

Common Modulation of the Motoric Pathway by STN-DBS and GPi-DBS

Within the classical cortico-striato-thalamic loop models, both the STN and GPi relay neural signals from the striatum and globus pallidus externus (GPe) forward to the thalamus (and back to the cortex).[36] The mainstream pathophysiological hypothesis explains PD symptoms as an abnormal increase in STN and GPi activity that in a net-sum effect would inhibit thalamic activity and, consequentially, decrease prokinetic cortical activity[37]; thus, the symptoms conceptually arise from an aberrant increase in the indirect pathway output via the GPe and a decrease in the direct pathway activity via the GPi, in which both mechanisms lead to the overinhibition of the thalamus and cortex under-activation. The primary finding of the present study is that functional connectivity between the somatosensory-motor cortices and thalamus negatively correlated with motor function improvement in both GPi-DBS and STN-DBS for PD, illustrating that, in humans, thalamocortical connections are a common pathway in subthalamic and pallidal stimulations for PD. In addition, our results showed that the cerebellum also showed altered connectivity under the STN-DBS and GPi-DBS. Our results are consistent with several recent studies using resting or task-based fMRI, suggesting that the activity or connectivity profile of the cerebellum is influenced by STN-DBS.[7,8,14]

The STN and GPi seem to play a similar role in sensorimotor, associative, and limbic domains of brain function. Clinical trials have indicated a similar degree of motor improvement between DBS at the 2 target sites.[2] Although several previous studies have illustrated the effect of STN-DBS on the brain dynamics in patients with PD,[4–7,9–15] our findings of the similar alterations in degree centrality and functional connectivity by DBS at the 2 nuclei suggest that STN-DBS and GPi-DBS have a similar modulatory effect on the motoric pathway. Crucially, the changes in thalamocortical functional connectivity are correlated (to a similar degree) with clinical improvements at both target sites.

VTA-GPi intersection volume was found, for the first time, to be correlated with alterations in functional connectivity between the somatosensory-motor cortices and the thalamus. This was also observed in patients with PD with STN-DBS, consistent with the findings in previous studies.[14,23] The correlation between the alterations in thalamocortical connectivity and VTA-nucleus

intersection was no longer significant after the inclusion of DBS-induced motor improvement as a covariate. These results suggest that thalamocortical functional connectivity is modulated by the accuracy of DBS targeting. In other words, the higher the proportion of the nucleus overlapping with VTA, the more the thalamocortical functional connectivity changes, which is associated with the motor improvement by DBS.

Dissociable Effects of STN-DBS Versus GPi-DBS on Brain Connections

Shen and colleagues proposed 2 distinct neurocircuits based on STN-DBS-induced activation versus deactivation in a block-design functional MRI: one involves the GPi, thalamus, and deep cerebellar nuclei (named GPi circuit); whereas the other involves the primary motor cortex, putamen, and cerebellum (named M1 circuit).[7] Our results indicate that both STN-DBS and GPi-DBS influenced the functional connectivity among the structures within the 2 neurocircuits. However, besides a similar modulatory effect on brain connectivity from STN- and GPi-DBS, our results also show that DBS-induced decreases in connectivity in more extensive regions in patients with STN-DBS than in patients with GPi-DBS. Notably, STN-DBS weakened functional connectivity between the cerebellum and postcentral gyrus and between the somatomotor network and visual network, whereas GPi-DBS did not. The differentiated impact on alterations in connectivity and motor improvement (STN-DBS was performed at a lower voltage but achieved better motor improvement than GPi-DBS; see the Table and Supplementary Table S3) may result from the anatomic differences between the STN and GPi. The volume of the GPi ($\sim$400 to 500 mm^3) is roughly 3 times that of the STN ($\sim$150 to 300 mm^3).[38] They use different neurotransmitters (GABA vs. glutamate),[39] and the cytoarchitecture may also have some target-specific modulation effects on distinct brain areas, as suggested in previous animal studies.[16,17] Moreover, developmentally, the STN is a caudal differentiation of the lateral hypothalamic area, whereas the GPi originates from the subpallial region.[40] Thus, although both GPi and STN are viable targets for motor symptoms, distinct therapeutic effects in certain aspects are non-negligible,[2,41] possibly resulting from the beneficial effect of the more expansive GPi region,[38] enabling more focal electric stimulation to sensorimotor functional subzones. Activation and deactivation in more extensive brain areas were shown with increasing stimulating STN-DBS voltage.[8] A previous randomized controlled trial comparing the DBS effect between 63 patients with STN-DBS and 62 patients with GPi-DBS also suggests more motor improvement by STN-DBS than GPi-DBS under the off-medication state.[42] Thus, the wider network

modulation of STN compared to that of GPi may be a hint for a more beneficial therapy or higher risk of side effects.

Our observation that only STN-DBS, but not GPi-DBS, weakened functional connectivity between the cerebellum and postcentral gyrus is consistent with the results from an animal study indicating that STN-DBS impacted a wider range of brain areas than GPi-DBS, including the somatosensory cortices and the cerebellum.[16] The cerebellar vermis showed an increased metabolism under STN-DBS,[43] and it was shown to be a key region in ataxia-related analysis and cognitive function.[44,45] The dissociable DBS-modulated connectivity observed in the present study could be a potential neural basis to explain the differences in clinical effects, such as the differentiated antidyskinetic effects and adverse effects related to posture, gait, and cognitive function.[2,46,47] The functional connectivity between the somatomotor network and visual network is associated with multimodal integration.[48,49] This connectivity decreased under STN-DBS but not GPi-DBS, which suggests multimodal integration may be selectively affected by STN-DBS. Further studies are needed to associate the differentiated alterations in connectivity with particular differences in clinical effects besides the UPDRS-III scores (eg, antidyskinesia effect, gait, speech, swallowing, mood, and cognitive functions) of DBS at the 2 target sites.

Limitations

This study has several limitations. First, the included patients had late-stage PD, and early-stage PD pathology may differ. Second, the sample size was relatively small, and the magnetic resonance field was relatively low due to safety concerns, which may have led to a relatively low statistical power. Thus, some negative results need to be evaluated in future studies with larger sample sizes and higher magnetic resonance fields. For instance, in the present study, the voxel-wise analyses did not reveal significant dissociable effects between DBS at 2 targets, so we further used ROI analysis to examine the potentially different effects. Third, owing to the evident signal loss of the functional images at and around the electrodes, the DBS-targeted nuclei were not chosen as ROIs, although a recent study examined the functional connectivity to the STN.[14] Fourth, inaccuracies in lead location by wrapping electrodes into a common space using the pipeline of Lead-DBS are possible, as discussed in a recent article.[50] Last, the patients were scanned in DBS-on state and thereafter rescanned approximately 60 minutes after switching off DBS. Hence, the results should be interpreted as network effects after "acute deactivation of chronic DBS." Network effects associated with acute DBS activation would require a protocol of either de novo activation of DBS in a DBS naive state after surgery or activation of DBS after a prolonged washout of at least 24 to 48 hours.

Conclusions

Three main conclusions may be drawn from this study. First, the functional connectivity between the somatosensory-motor cortices and thalamus, and that between the somatosensory-motor cortices and cerebellum decreased in the DBS-on state versus the off state. Further, DBS-modulated connectivity between the somatosensory-motor cortices and thalamus correlated with motor improvement induced by both STN- and GPi-DBS. Second, DBS-induced changes in thalamocortical connectivity were modulated by the intersection volume of nucleus and estimated VTA in both STN- and GPi-DBS, and associated with motor improvement under DBS. Third, the subthalamic stimulation modulated the functional connectivity among a wider range of brain areas than the pallidal stimulation, and particularly interactions were observed between DBS of the STN and GPi in motor-related cortical and cerebellar areas, and in somatomotor and visual networks, suggesting differentiated neural modulations of the 2 target sites. Further studies are needed to determine whether the dissociable alterations in connectivity under STN- and GPi-DBS are the underlying neural basis for the different clinical effects of DBS at these 2 target sites. Thus, our findings contribute to the understanding of the mechanisms of action of DBS at a system level, highlighting the common and specific effects of STN-DBS and GPi-DBS on functional connectivity in patients with PD, which potentially underlie their similar, but not identical, neural modulations. Our results provide mechanistic insight and potential to refine target selection strategies for focal brain stimulation in PD.

Author Contributions

C.C.Z., D.Y.L., F.H.Y., and B.M.S. contributed to the conception and design of the study. C.C.Z., N.Y.H., Yu. L., Yan.L., D.Y.L., Y.J.L., H.Y.L., and J.L. contributed to the acquisition and analysis of data. C.C.Z., J.L., Y.J.L, H.J.W., and A.H. contributed to drafting the text or preparing the figures.

Potential Conflicts of Interest

The authors report no competing interests.

References

1. Obeso JA, Rodriguez-Oroz MC, Benitez-Temino B, et al. Functional organization of the basal ganglia: therapeutic implications for Parkinson's disease. Mov Disord 2008;23:S548–S559.

2. Ramirez-Zamora A, Ostrem JL. Globus pallidus interna or subthalamic nucleus deep brain stimulation for Parkinson disease: a review. JAMA Neurol 2018;75:367–372.

3. Zhang C, Wang L, Hu W, et al. Combined unilateral subthalamic nucleus and contralateral globus pallidus interna deep brain stimulation for treatment of Parkinson disease: a pilot study of symptom-tailored stimulation. Neurosurgery 2020;87:1139–1147. https://doi.org/10.1093/neuros/nyaa201

4. Phillips MD, Baker KB, Lowe MJ, et al. Parkinson disease: pattern of functional MR imaging activation during deep brain stimulation of subthalamic nucleus—initial experience. Radiology 2006;239:209–216.

5. Jech R, Urgosik D, Tintera J, et al. Functional magnetic resonance imaging during deep brain stimulation: a pilot study in four patients with Parkinson's disease. Mov Disord 2001;16:1126–1132.

6. Knight EJ, Testini P, Min HK, et al. Motor and nonmotor circuitry activation induced by subthalamic nucleus deep brain stimulation in patients with Parkinson disease: intraoperative functional magnetic resonance imaging for deep brain stimulation. Mayo Clin Proc 2015;90:773–785.

7. Shen L, Jiang C, Hubbard CS, et al. Subthalamic nucleus deep brain stimulation modulates 2 distinct Neurocircuits. Ann Neurol 2020;88:1178–1193.

8. Boutet A, Madhavan R, Elias GJB, et al. Predicting optimal deep brain stimulation parameters for Parkinson's disease using functional MRI and machine learning. Nat Commun 2021;12:3043.

9. Mueller K, Jech R, Ruzicka F, et al. Brain connectivity changes when comparing effects of subthalamic deep brain stimulation with levodopa treatment in Parkinson's disease. Neuroimage Clin 2018;19:1025–1035.

10. Mueller K, Jech R, Schroeter ML. Deep-brain stimulation for Parkinson's disease. N Engl J Med 2013;368:482–483.

11. Holiga S, Mueller K, Moller HE, et al. Resting-state functional magnetic resonance imaging of the subthalamic microlesion and stimulation effects in Parkinson's disease: indications of a principal role of the brainstem. Neuroimage Clin 2015;9:264–274.

12. Kahan J, Mancini L, Urner M, et al. Therapeutic subthalamic nucleus deep brain stimulation reverses cortico-thalamic coupling during voluntary movements in Parkinson's disease. PLoS One 2012;7:e50270.

13. Kahan J, Urner M, Moran R, et al. Resting state functional MRI in Parkinson's disease: the impact of deep brain stimulation on 'effective' connectivity. Brain 2014;137:1130–1144.

14. Horn A, Wenzel G, Irmen F, et al. Deep brain stimulation induced normalization of the human functional connectome in Parkinson's disease. Brain 2019;142:3129–3143.

15. Saenger VM, Kahan J, Foltynie T, et al. Uncovering the underlying mechanisms and whole-brain dynamics of deep brain stimulation for Parkinson's disease. Sci Rep 2017;7:9882.

16. Min HK, Hwang SC, Marsh MP, et al. Deep brain stimulation induces BOLD activation in motor and non-motor networks: an fMRI comparison study of STN and EN/GPi DBS in large animals. Neuroimage 2012;63:1408–1420.

17. Lai HY, Younce JR, Albaugh DL, et al. Functional MRI reveals frequency-dependent responses during deep brain stimulation at the subthalamic nucleus or internal globus pallidus. Neuroimage 2014;84:11–18.

18. Vitek JL, Johnson LA. Understanding Parkinson's disease and deep brain stimulation: role of monkey models. Proc Natl Acad Sci U S A 2019;116:26259–26265.

19. McFarland NR, Haber SN. Thalamic relay nuclei of the basal ganglia form both reciprocal and nonreciprocal cortical connections, linking multiple frontal cortical areas. J Neurosci 2002;22:8117–8132.

20. Bosch-Bouju C, Hyland BI, Parr-Brownlie LC. Motor thalamus integration of cortical, cerebellar and basal ganglia information: implications for normal and parkinsonian conditions. Front Comput Neurosci 2013;7:163.

21. Thirion B, Pinel P, Meriaux S, et al. Analysis of a large fMRI cohort: statistical and methodological issues for group analyses. Neuroimage 2007;35:105–120.

22. Goetz CG, Tilley BC, Shaftman SR, et al. Movement Disorder Society-sponsored revision of the unified Parkinson's disease rating scale (MDS-UPDRS): scale presentation and clinimetric testing results. Mov Disord 2008;23:2129–2170.

23. Horn A, Li N, Dembek TA, et al. Lead-DBS v2: towards a comprehensive pipeline for deep brain stimulation imaging. Neuroimage 2019;184:293–316.

24. Penny WD, Friston KJ, Ashburner JT, et al. Statistical parametric mapping: the analysis of functional brain images. Amsterdam: Elsevier, 2011.

25. Schonecker T, Kupsch A, Kuhn AA, et al. Automated optimization of subcortical cerebral MR imaging-atlas coregistration for improved postoperative electrode localization in deep brain stimulation. AJNR Am J Neuroradiol 2009;30:1914–1921.

26. Fonov V, Evans A, McKinstry R, et al. Unbiased nonlinear average age-appropriate brain templates from birth to adulthood. NeuroImage 2009;47:S102.

27. Avants BB, Epstein CL, Grossman M, Gee JC. Symmetric diffeomorphic image registration with cross-correlation: evaluating automated labeling of elderly and neurodegenerative brain. Med Image Anal 2008;12:26–41.

28. Horn A, Reich M, Vorwerk J, et al. Connectivity predicts deep brain stimulation outcome in Parkinson disease. Ann Neurol 2017;82:67–78.

29. Ewert S, Plettig P, Li N, et al. Toward defining deep brain stimulation targets in MNI space: a subcortical atlas based on multimodal MRI, histology and structural connectivity. Neuroimage 2018;170:271–282.

30. Yan CG, Wang XD, Zuo XN, Zang YF. DPABI: data processing & analysis for (resting-state) brain imaging. Neuroinformatics 2016;14:339–351.

31. Ashburner J, Friston KJ. Diffeomorphic registration using geodesic shooting and Gauss-Newton optimisation. Neuroimage 2011;55:954–967.

32. Friston KJ, Williams S, Howard R, et al. Movement-related effects in fMRI time-series. Magn Reson Med 1996;35:346–355.

33. Rubinov M, Sporns O. Complex network measures of brain connectivity: uses and interpretations. Neuroimage 2010;52:1059–1069.

34. Rolls ET, Huang CC, Lin CP, et al. Automated anatomical labelling atlas 3. Neuroimage 2020;206:116189.

35. Li X, Xing Y, Martin-Bastida A, et al. Patterns of grey matter loss associated with motor subscores in early Parkinson's disease. Neuroimage Clin 2018;17:498–504.

36. Nambu A. A new dynamic model of the cortico-basal ganglia loop. Prog Brain Res 2004;143:461–466.

37. Wichmann T, DeLong MR. Pathophysiology of Parkinson's disease: the MPTP primate model of the human disorder. Ann N Y Acad Sci 2003;991:199–213.

38. Mulder MJ, Keuken MC, Bazin P-L, et al. Size and shape matter: the impact of voxel geometry on the identification of small nuclei. PLoS One 2019;14:e0215382.

39. Galvan A, Kuwajima M, Smith YJN. Glutamate and GABA receptors and transporters in the basal ganglia: what does their subsynaptic localization reveal about their function? Neuroscience 2006;143:351–375.

40. Swanson LW. Cerebral hemisphere regulation of motivated behavior. Brain Res 2000;886:113–164.

41. Au KLK, Wong JK, Tsuboi T, et al. Globus pallidus internus (GPi) deep brain stimulation for Parkinson's disease: expert review and commentary. Neurol Ther 2020;10:7–30.

42. Odekerken VJ, van Laar T, Staal MJ, et al. Subthalamic nucleus versus globus pallidus bilateral deep brain stimulation for advanced Parkinson's disease (NSTAPS study): a randomised controlled trial. Lancet Neurol 2013;12:37–44.

43. Asanuma K, Tang C, Ma Y, et al. Network modulation in the treatment of Parkinson's disease. Brain 2006;129:2667–2678.

44. Reich MM, Brumberg J, Pozzi NG, et al. Progressive gait ataxia following deep brain stimulation for essential tremor: adverse effect or lack of efficacy? Brain 2016;139:2948–2956.

45. Huang C, Mattis P, Tang C, et al. Metabolic brain networks associated with cognitive function in Parkinson's disease. Neuroimage 2007;34:714–723.

46. Coffman KA, Dum RP, Strick PL. Cerebellar vermis is a target of projections from the motor areas in the cerebral cortex. Proc Natl Acad Sci U S A 2011;108:16068–16073.

47. Zhang Y, Yang Y, Yang Y, et al. Alterations in cerebellar functional connectivity are correlated with decreased psychomotor vigilance following total sleep deprivation. Front Neurosci 2019;13:134.

48. Shipp S, Blanton M, Zeki S. A visuo-somatomotor pathway through superior parietal cortex in the macaque monkey: cortical connections of areas V6 and V6A. Eur J Neurosci 1998;10:3171–3193.

49. Ding C, Palmer CJ, Hohwy J, et al. Deep brain stimulation for Parkinson's disease changes perception in the rubber hand illusion. Sci Rep 2018;8:13842.

50. Li N, Baldermann JC, Kibleur A, et al. A unified connectomic target for deep brain stimulation in obsessive-compulsive disorder. Nat Commun 2020;11:3364.